AD-A056 488 WATERVLIET ARSENAL N Y BENET WEAPONS LAB F/G 19/6
RADIAL AND TRANSVERSE RESPONSE OF GUN TUBES TO TRAVELING BALLIS--ETC(U)
JUN 78 T E SIMKINS, R D SCANLON, G A PFLEGL

UNCLASSIFIED NL

| OF |
AD
A056488

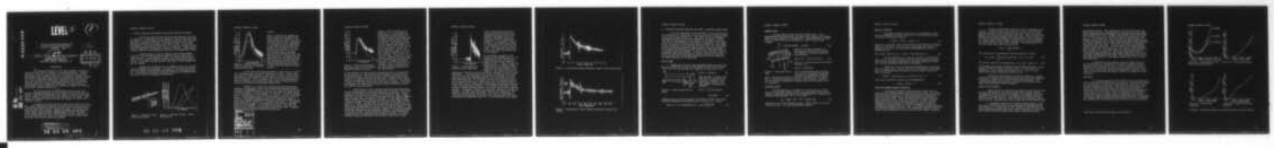

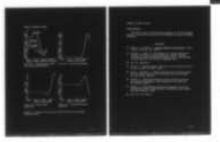

END
DATE
FILMED
8 -78
DDC

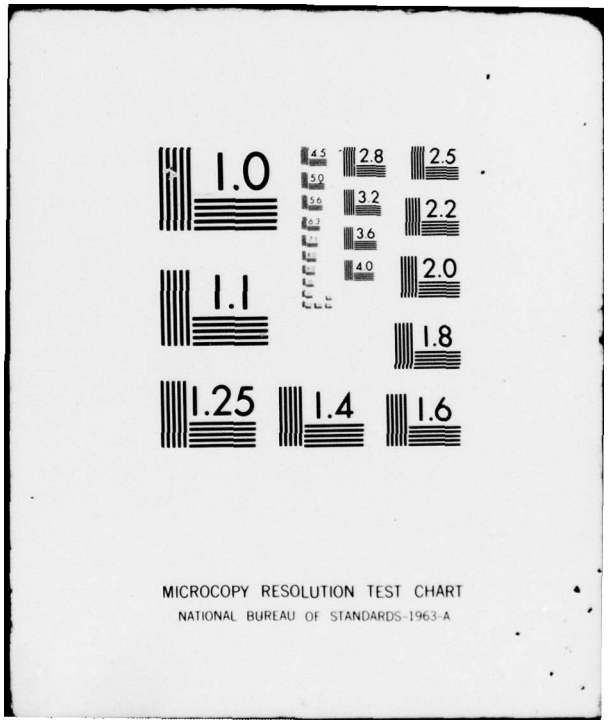
1.0
1.1
1.25
1.4
1.6
1.8
2.0
2.2
2.5
2.8
3.2
3.6
4.0
4.5
5.0
5.6
MICROCOPY RESOLUTION TEST CHART
NATIONAL BUREAU OF STANDARDS-1963-A

LEVEL II

1

RADIAL AND TRANSVERSE RESPONSE OF GUN TUBES TO TRAVELING BALLISTIC PRESSURE, (U)

14p.

JUN 1978

THOMAS E. SIMKINS, RAYMOND D. SCANLON, MR.
GEORGE A. PFLEGL, MR.
BENET WEAPONS LABORATORY
WATERVLIET ARSENAL, WATERVLIET, NY

INTRODUCTION

The design and analysis of gun tubes presently proceeds on the basis of the static equations of continuum mechanics. Stresses within the tube wall, for example, are calculated by the classical Lame formula (1) - generally viewed as a conservative design criterion. The advent of high speed computation and mathematical modeling, however, has revealed that dynamic bore expansion during the interior ballistic cycle will create significantly higher wall stresses than those on which the tube design is based (2). The analytical and experimental results leading to this conclusion comprise the material in the first section of this work.

The second portion of the work which follows shows how transient bending vibrations may arise during firing due to tube curvature. Tube motions predicted at the muzzle are of sufficient magnitude to explain a portion of the error realized at the target. Three sources of curvature-induced vibration are derived (3) and two are treated in detail.

An appreciable effort has been made in the interest of realism. Highly detailed tube geometries and interior ballistic curves of pressure and projectile travel for specific weapons of interest have been included in the analysis. Wherever possible, use has been made of the large, widely accepted, NASTRAN (NAsa STRuctural ANalysis) finite element computer code. Though NASTRAN is quite versatile, it is not particularly well suited for handling curvature-induced load functions which require special programming.

371 075

SIMKINS, SCANLON & PFLEGL

1. RADIAL VIBRATIONS IN RESPONSE TO TRAVELING BALLISTIC PRESSURE

The 175 mm, M113 gun tube was chosen for analysis. The tube is assumed to be completely free of supports, closed at the breech and subjected to a time-variant internal ballistic pressure which traverses the bore at projectile velocity. Of primary interest is the radial displacement of the bore surface of the tube in time. To this end a 250 degree-of-freedom model of the tube is created by dividing the tube into 62 trapezoidal ring elements as shown in Figure 1. These finite elements allow the true geometry of the tube to be modeled very closely.

Program output in terms of radial or axial displacements, velocities, or accelerations may be requested for any bore station along the tube. As representative output, the radial displacement vs. time at three locations along the tube have been selected for presentation. In all there are 125 points in the model at which program output is computed.

Geometrical information for the NASTRAN program was obtained from tube manufacturing drawings. Tabulations of the pressure-travel curves of Figure 2 provided the input necessary for load specification (4). Traveling loads cannot be prescribed directly for NASTRAN input and require special programming considerations.

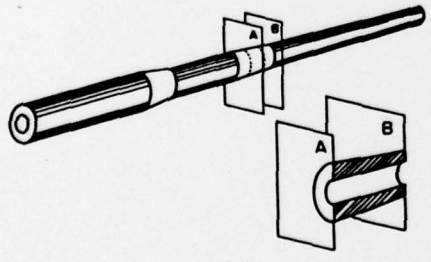

Figure 1 - Section of Trapezoidal Ring Element.

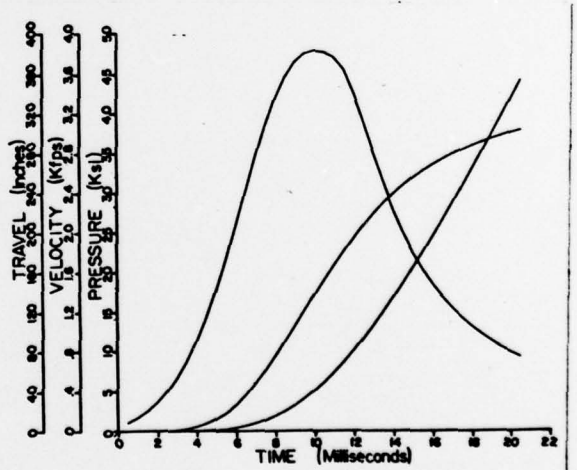

Figure 2 - Ballistic Curves - 175 mm M113 (Zone 3).

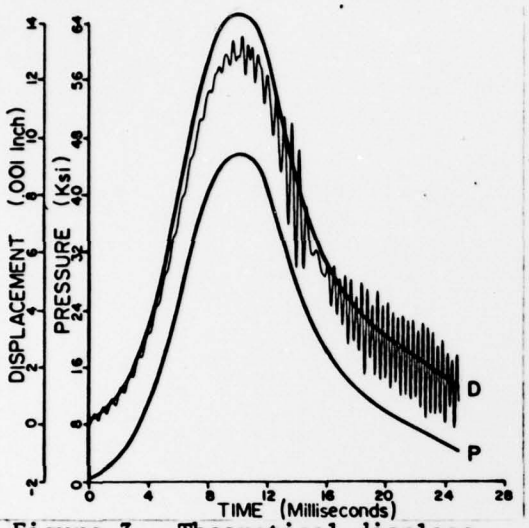

Figure 3 - Theoretical displacement and pressure in the breech section of the tube.

RESULTS

Figure 3 displays the NASTRAN-predicted radial displacement of the bore surface at a location in the breech of the gun tube. Superposed for comparison is the displacement as calculated from the Lame design formula and the applied pressure. Owing to its location to the rear of the projectile at all times, this station receives pressure smoothly and continuously from time zero (ignition). Consequently, the loading rate at this point depends only on the rate at which the burning propellant produces pressure and not primarily upon the velocity at which the load follows the projectile.

It may also be observed from figure 3 that there is a steadily increasing amount of natural frequency excitation. These vibrations have a visible tendency to form 'beats' in the classical sense and infer the coexistence of several modes of vibration having nearly equal frequencies. Their importance lies in that the amplitudes of the beat envelopes can attain quite large values, creating an opportunity for overstress and shortened fatigue life.

Finally, it is noted that the Lame-predicted displacement response is conservative in that its maximum value exceeds that predicted by the NASTRAN analysis. This is to be expected since the Lame solution is formed on the assumption that the tube is uniformly pressurized throughout its entire length. In reality - and in the NASTRAN model - the pressure only exists in the region to the rear of the projectile. The unloaded region in front of the projectile tends to assume its unloaded configuration exerting a contractile effort on the pressurized region to the rear. Only when there exists a considerable input of kinetic energy to a given mode of vibration will the Lame prediction be exceeded. It is evident from figure 3 that this condition is not fulfilled in the breech section of the tube. Different behavior will be witnessed further along the bore.

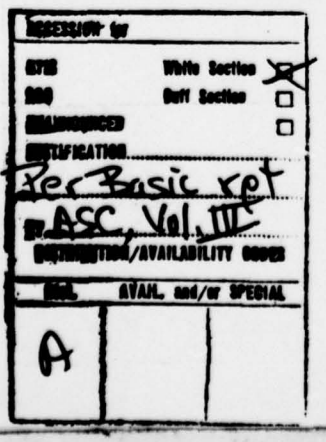

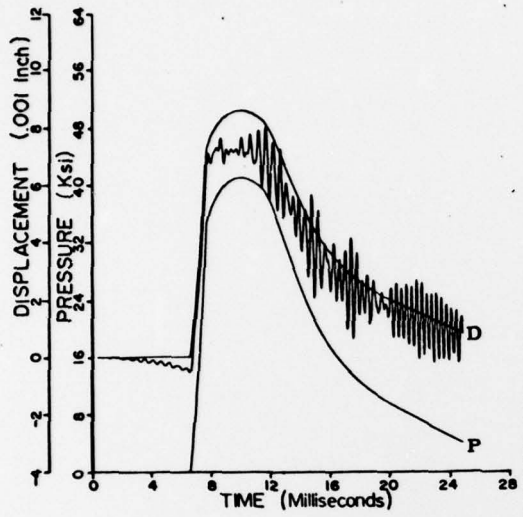

Figure 4 - Theoretical Displacement and Pressure a Short Distance Beyond the Origin of Rifling.

Figure 4 shows the same set of functions, i.e., the NASTRAN and Lamé predicted displacements and the applied ballistic pressure, at a station located a short distance in front of the projectile prior to ignition. The distinctive feature as compared with Figure 3 is the time delay prior to the arrival of the projectile. During this delay a negative, that is, an inward radial displacement occurs at this location. This is the 'contractile effect' referred to in the previous paragraph, caused by adjacent regions of pressure and non-pressure. The Lame calculation cannot, of course, account for such an effect since all regions are assumed uniformly pressurized in the Lame problem.

At approximately 6.5 milliseconds following ignition, the projectile passes exposing this portion of the bore surface to the pressure of the propellant gas. Thus the time rate of load application at this station, in contrast with that in the breech, is almost wholly determined by the magnitude of the load velocity at this time. The loading is seen to be much more abrupt than that shown in Figure 3. This notwithstanding, one notes that the Lame-calculated displacement proves once again to be conservative.

While Figures 3 and 4 show the Lamé-calculated displacement to err conservatively at bore locations nearer the breech, this is not typical of the behavior at stations further along the bore. Figure 5 represents the response more likely to be realized at least at some down bore locations. The station represented in this figure is approximately midway along the length of the tube. At this point the projectile is moving with a very high velocity and a very abrupt loading condition results. Provided that the vibration of the surface is in phase (i.e., moving outward) with the pressure application, a relatively large radial displacement will result as is the case in Figure 5. One should note that only a short distance forward and aft of this location the surface movement may be completely reversed. A sudden application of pressure at these locations would do negative work on the moving surface and the oscillations may be greatly attenuated. The actual locations along the tube where one can expect overstresses (large

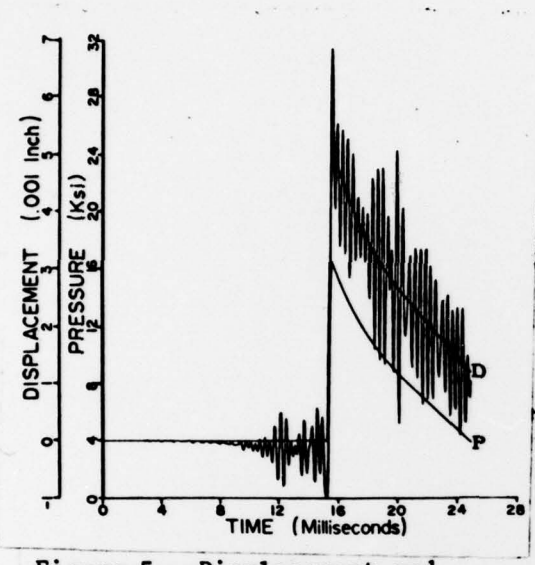

Figure 5 - Displacement and pressure midway along tube

radial displacements beyond the Lame prediction) cannot really be computed accurately owing to the imperfect knowledge of the true boundary conditions and material properties - not to mention the inability of any integration scheme to follow the phase accurately over a great number of cycles of vibration. It is important nonetheless to know that such overstresses are to be expected.

As experimental evidence of the success of the NASTRAN analysis, two representative test records from actual gun firings are offered in figures 6 and 7. Figure 6 shows the displacement at a location midway along the tube and therefore can be compared semi-quantitatively with figure 5. One clearly observes the production of natural oscillations and the formation of beats of large amplitudes. It is mostly due to the absence of damping in the analysis and the greater abundance of modes in the real tube into which energy may flow, that the amplitudes in the test records are lesser than those predicted. It is notable that the time-averaged displacement estimated from figure 6 agrees quite well with that of figure 5. On the other hand the excessively large maximum displacement of figure 5 does not materialize in figure 6. As previously discussed, this is a matter of phase agreement between the surface motion and the applied pressure. In figure 7, however, an overstress condition is clearly in evidence - the peak Lame value being indicated for comparison. This station is located nearer the muzzle. One notes the exceptionally clear oscillation and beat formations which continue after shot ejection which is estimated to occur at t = 21 milliseconds in the figure.

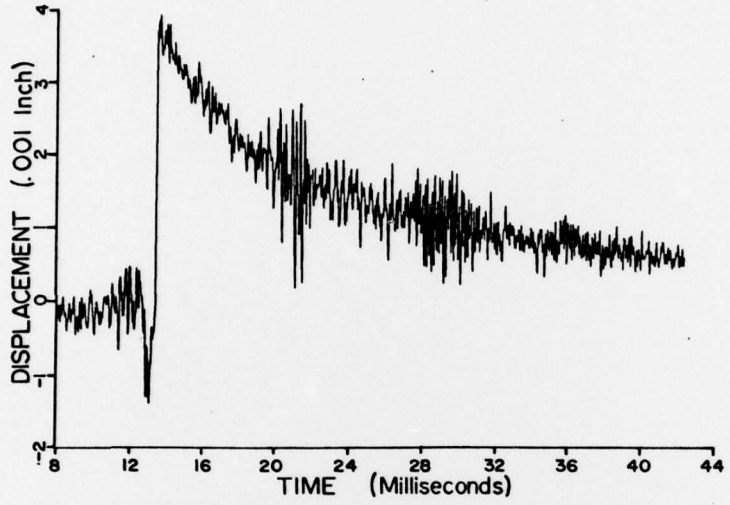

Figure 6 - Displacement Midway Along Tube Length (Actual Test Firing).

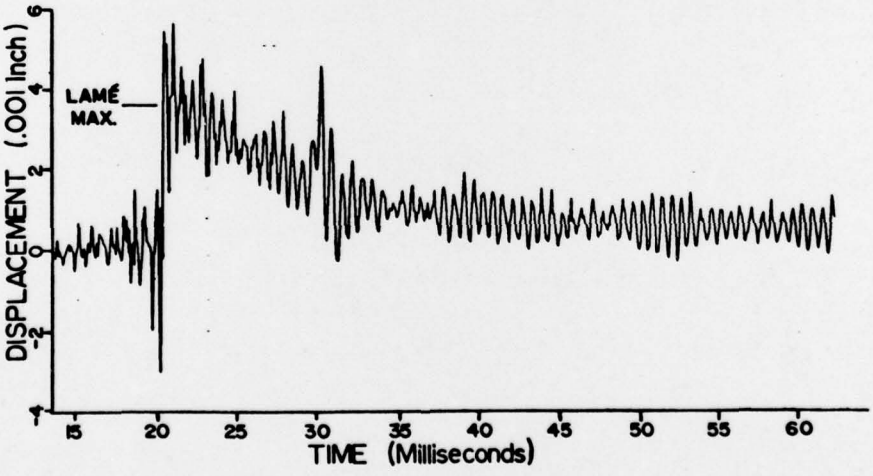

Figure 7 - Displacement a Short Distance From Muzzle (Actual Test Firing)

2. TRANSVERSE (BENDING) MOTION OF GUN TUBES - CURVATURE INDUCED LOADS

In 1959, measurements by Gay and Elder of the US Army Ballistics Laboratory (5) showed that the muzzle motions of a 90 mm tank gun at the time of shot ejection are very small but yet significant in explaining a portion of the error realized at the target. Typical rotations and displacements at the muzzle, for example, were of the order of 10^{-1} milliradians and 10^{-2} inches, respectively. The theory of gun tube motion by which explanations were sought for these observations assumed that the motion was due solely to a mass eccentricity at the breech which produced a sudden inertial moment upon recoil. The theoretically predicted motion, however, was often much smaller in magnitude than that observed. In the work that follows it will be shown that loads resulting from the initial curvature of the M-68, 105 mm gun tube can also produce muzzle motions of these magnitudes and should therefore not be neglected.

Recoil Loads

During the recoil of a gun tube there results an axial load per unit length which is equal to the product of the recoil acceleration, $\alpha(t)$, and the mass per unit length of the tube $\rho(x)$; i.e.,

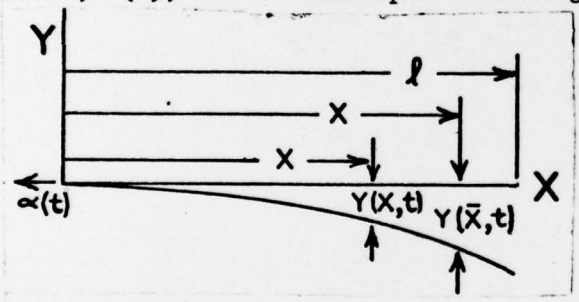

Figure 8 - Inertial Moment Due to Recoil.

$$w(x,t) = -\rho(x)\alpha(t) \qquad (1)$$

When the tube is curved, this load creates a moment at any location x, along the tube. Referring to Figure 8, the total moment is given by the integral:

$$M(x,t) = \int_x^{\ell} -w(\bar{x},t)[y(\bar{x},t) - y(x,t)]d\bar{x} \qquad (2)$$

Differentiating twice with respect to the space variable x gives the resultant transverse load intensity due to recoil: [(') = $\partial/\partial x$]

$$f_R(x,y',y'',t) = \alpha(t)\{\rho(x)y'(x,t) - y''(x,t)\int_x^{\ell}\rho(\xi)d\xi\} \qquad (3)$$

'Bourdon' Load

If a gun tube is curved, the bore surface area becomes asymmetrically distributed about the central axis owing to the relative extension and contraction of the material. From the geometry of Figure 9 one can verify that the net difference in area is given by the integral:

$$\int_0^{2\pi} (\sin\Theta+1)a\sin\Theta d\Theta dx = -\pi a^2 y'' dx \qquad (4)$$

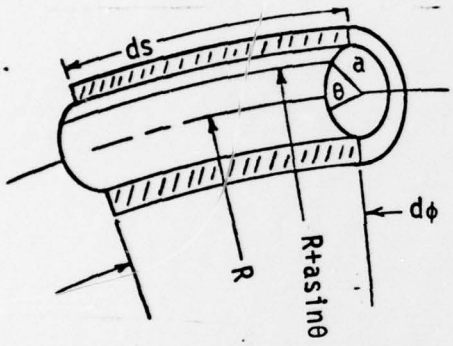

Figure 9 - Curved Section of Tube.

where R^{-1} has been replaced by $-y''$. The applied ballistic pressure therefore produces a resultant transverse load intensity:

$$f_B(x,y'',t) = -p(x,t)\pi a^2 y''(x,t) \qquad (5)$$

$p(x,t)$ is a traveling ballistic pressure function, i.e.,

$$p(x,t) = P_o(t)H(\xi-x)$$

$H(z)$ is the Heaviside unit step function and $\xi(t)$ represents the distance traveled by the projectile along the bore. (f_B has been called the 'Bourdon' Load because of its similarity to a straightening Bourdon tube upon pressurization. Actually, the two effects are completely different and the term 'Bourdon' load is a misnomer.)

Projectile Loads

If the projectile is assumed to be a point mass m_p, traveling a bore path which changes in time, it can be shown (8) that there results a transverse load function containing Coriolis, centrifugal and transverse accelerations, i.e., [$(\cdot) = \partial/\partial t$]

$$f_p = -m_p[\ddot{y} + 2V\dot{y}' + V^2y'' + g]\delta(x-\xi(t)) \qquad (6)$$

where $\delta(z)$ is the Dirac function and $\xi(t) = \int_0^t V dt$, where V is the projectile velocity. g is the gravitational constant.

Equation of Motion

Using Euler-Bernoulli beam theory, the displacement $y(x,t)$ from the undeformed (straight) neutral axis of the tube must satisfy the partial differential equation:

$$(EIy'')'' + \rho(x)\ddot{y} - f - (EIY'')'' = 0 \tag{7}$$

where $I(x)$ is the area cross section moment of inertia and E is Young's Modulus of Elasticity. The last term on the right hand side of (7) represents the static load intensity corresponding to an initial deformation $Y(x)$.

The initial conditions are: $y(x,0) = Y(x)$ and $\dot{y}(x,0) = 0$ (8)

The load functions $f = f_R$ and $f = f_B$ will be considered in turn. It is to be noted, however, that the beam motions due to each load function may <u>not</u> be superposed as the linear operators involved vary with the particular load function considered.

Taking $Y(x)$ to be the gravitational deformation of the tube prior to firing, and $f = f_R(x,y',y''t)$ it is convenient to first define $\bar{y}(x,t)$ as the displacement as measured from the initial curve $Y(x)$. Thus (7) becomes:

$$(EI\bar{y}'')'' + \rho(x)\ddot{\bar{y}} - f_R(\bar{y},\bar{y}'',x,t) - f(Y',Y'',x,t) = 0 \tag{9}$$

The initial conditions in terms of $\bar{y}$ are homogeneous:

$$\bar{y}(x,0) = \dot{\bar{y}}(x,0) = 0 \tag{10}$$

Static and Dynamic Support Conditions

The support (boundary) conditions which prevail prior to firing may not be appropriate during the ballistic cycle. For the purpose of calculating the initial static gravitational deformation $Y(x)$, the M-68 tube is assumed to be cantilevered from its two mounting points near the breech. Actual vibration records indicate that the mount connections are far from rigid, however. In fact, excellent agreement between calculated and experimentally observed natural frequencies is obtained only if the tube is regarded as virtually unsupported during the ballistic cycle. The dynamic boundary conditions are therefore assumed to be free. This assumption should be valid as long as tube displacements are of the order of the support clearances.

The partial differential equation (9) was transformed into a set of N - ordinary differential equations in time via the Galerkin procedure in which the basis functions were chosen to be the natural modes of vibration of the unsupported M-68 tube. Using once again the NASTRAN finite element program, these mode shapes, $W_i(x)$- as well as the initial gravitational deformation function $Y(x)$ - were determined at nineteen points along the tube. Between these points the shapes were interpolated by cubic spline functions. The approximation for $\bar{y}$ in terms of the mode shapes may be written:

$$\bar{y}(x,t) = \sum_{i=1}^{N} a_i(t)W_i(x) \quad ,$$

the resulting set of differential equations appear as follows:

$$\ddot{a}_i + \omega_i^2 a_i + \sum_{j=1}^{N} (A_{ij}(t)-B_{ij}(t))a_j = C_i(t);\ i=1 \text{ to } N \qquad (11)$$

The initial conditions are homogeneous, i.e., $a_i(0) = \dot{a}_i(0) = 0$ (12)

ω_i represents the natural frequency of the ith vibration mode. $A_{ij}(t)$ derives from the $\bar{y}''$ terms in (9) while $B_{ij}(t)$ reflects the slope dependency, $\bar{y}'$, and vanishes for the case $f = f_B$. $C_i(t)$ is due to terms in the initial deformation function $Y(x)$.

The system represented by (11) and (12) above, was solved numerically using 4th order, variable time step Runge Kutta integration. In practice a value of N = 10 gave satisfactory convergence. This included two rigid body modes (plane rotation and translation) and eight vibration modes of finite frequency.

RESULTS AND DISCUSSION

Figures 10 and 11 represent the response of the M-68 gun tube to recoil and asymmetric ballistic pressure (the 'Bourdon' effect). The magnitudes shown in each of the figures are comparable with those predicted by Gay and Elder (8) in connection with eccentric breech inertia in the T-139 tank gun. This indicates that curvature-induced loads should be included in any theory of gun tube motion during firing.

A fundamental difference is apparent between figures 10 and 11, and is especially obvious in comparing the time histories of the tube shapes, i.e., figures 10a and 11a. Whereas in 10a the motion is well developed along the entire tube length, the motion in 11a is much more wavelike and muzzle displacements remain comparatively small

through shot ejection. This difference is due to the fact that the recoil inertia load acts instantaneously* over the entire tube length whereas development of the 'Bourdon' load proceeds at projectile velocity. Moreover, the recoil loading consists of two parts (cf. equation 3). If evaluated near time zero, these two parts consist of a downward load proportional to the curvature (y") and therefore stronger near the supports, and an upward load proportional to the slope (y') more intense near the muzzle. The two act in unison to encourage a rotation of the entire tube. The large mass at the breech, however, tends to anchor that end of the tube. The result is the deformation shown in figure 10a. The Bourdon load, on the other hand, consists of only one part (cf. equation 5). This part, being proportional to curvature is greatest near the supports and trails off to practically zero value by mid-length of the tube. Muzzle displacement must therefore await the arrival of a disturbance originating from the support end of the tube.

A similarity is also apparent comparing figures 10 and 11. The time histories of the slopes at the muzzle - probably the most important of all the response curves - show a definite similarity in that little muzzle rotation occurs during the first half of the ballistic cycle. This delay represents the propagation time for a disturbance established near the supports (where y" is largest) to reach the muzzle.

CONCLUSION

To completely account for the motions of a gun tube prior to shot ejection several effects must be considered, among them the effects of tube curvature. Of particular significance is the muzzle slope at the time the projectile arrives. Slope values are particularly sensitive to sudden disturbances which originate near the support or breech end of the tube and propagate in wavelike fashion reaching the muzzle prior to shot ejection. This is exemplified in the case of the Bourdon load and strongly suggests an opportunity for further study as the supports themselves may create strong forces as clearances are abruptly taken up during the initial phases of recoil. The result may significantly strengthen rotations of the muzzle at shot ejection.

*The tube is assumed axially rigid in the analysis.

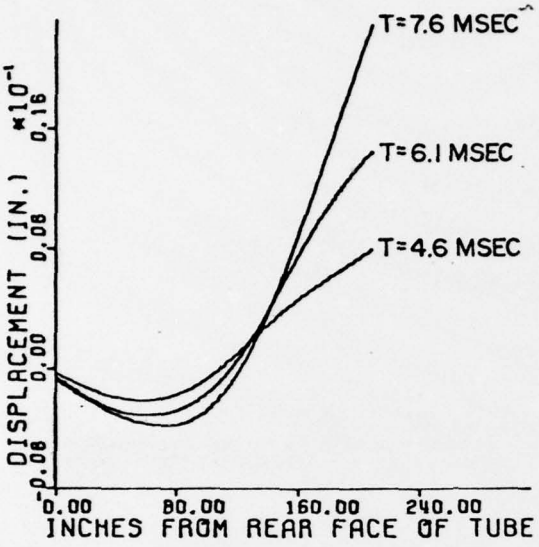

Figure 10a - Displacement of Tube Axis from Initial Position.

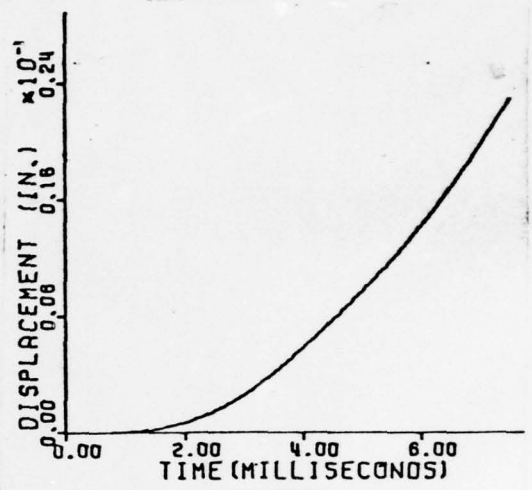

Figure 10b - Muzzle Displacement.

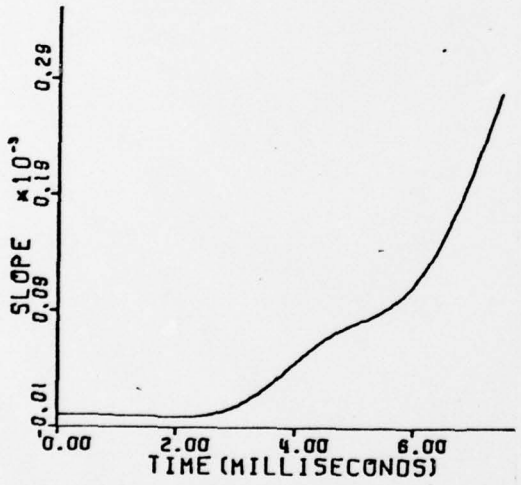

Figure 10c - Muzzle Slope (Rotation).

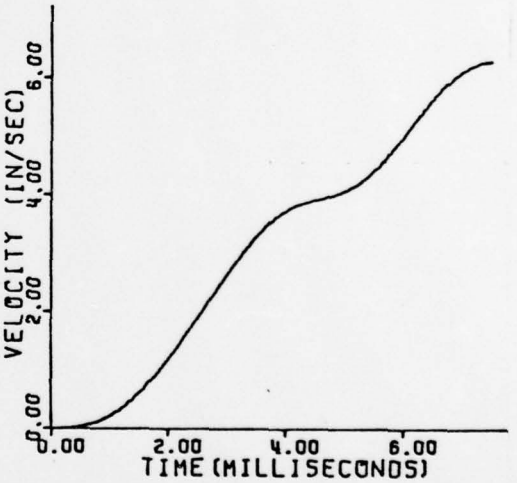

Figure 10d - Transverse Velocity of Muzzle.

Figure 10 - Transverse Response of the M-68 Gun Tube to Recoil Inertia.

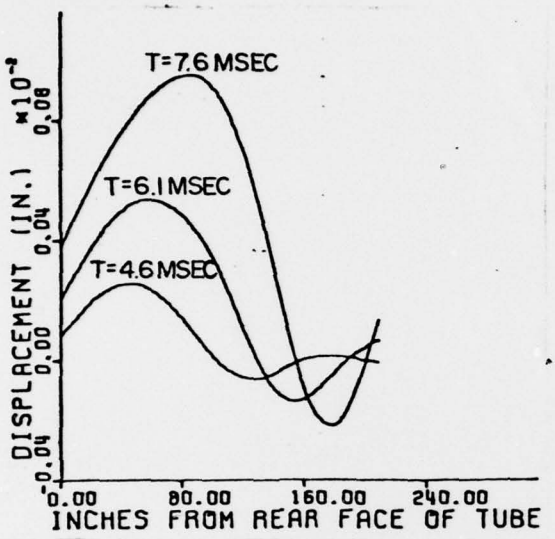

Figure 11a - Displacement of Tube Axis from Initial Position.

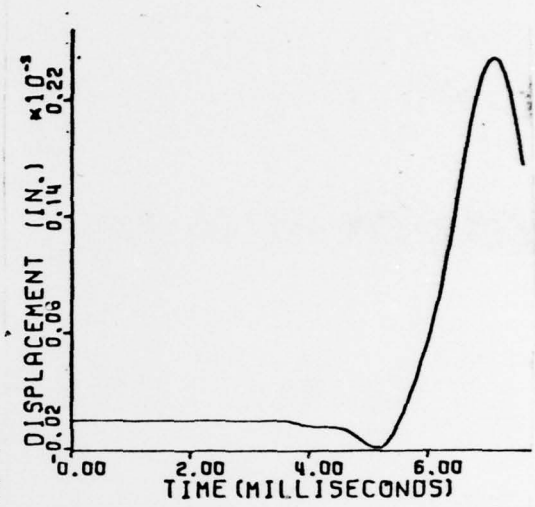

Figure 11b - Muzzle Displacement.

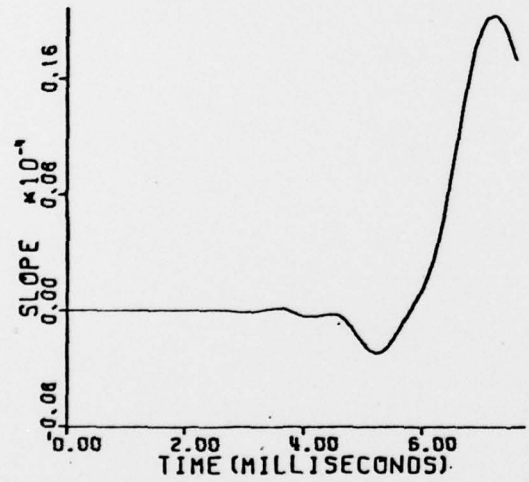

Figure 11c - Muzzle Slope (Rotation).

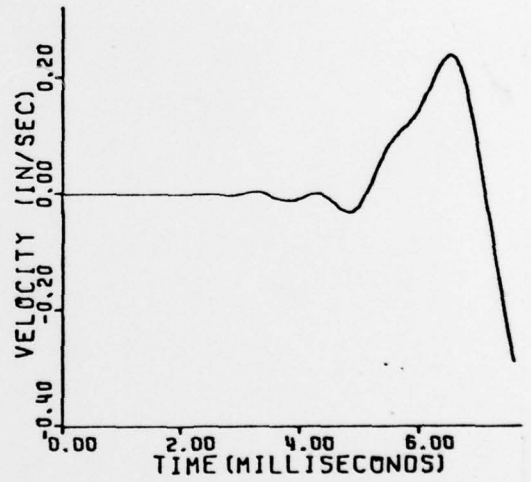

Figure 11d - Transverse Velocity of Muzzle.

Figure 11 - Transverse Response of the M-68 Gun Tube to Traveling Bourdon Pressure.

ACKNOWLEDGMENT:

The authors wish to thank Mr Richard Haggerty of the Benet Weapons Computer Science Laboratory and Miss Ellen Fogarty for their invaluable assistance.

REFERENCES

(1) Seeley, F. and Smith, J., Advanced Mechanics of Materials, 2nd Ed. (Wiley & Sons, NY), pp. 298-99.

(2) Simkins, T., Pflegl, G., and Scanlon, R., "Dynamic Response of the M113 Gun Tube to Travelling Ballistic Pressure and Data Smoothing as Applied to XM150 Acceleration Data" - Benet Weapons Lab Tech Report No. WVT-TR-75015, ADA010662 (1975)

(3) Ref. (2), Appendix B.

(4) Vottis, P., "Digital Computer Simulation of the Interior Ballistic Process in Guns", WVT-6615, (1966).

(5) Gay, H., and Elder, A., "The Lateral Motion of a Tank Gun and Its Effect on the Accuracy of Fire", Ballistic Research Lab Report No. 1070 (1959), AD217657.

(6) Simkins, T., "Structural Response to Moving Projectile Mass by the Finite Element Method," Benet Weapons Lab Tech Report No. WVT-TR-75044, (1975).

(7) Simkins, T., "Unconstrained Variational Statements for Initial and Boundary-Initial Value Problems", (forthcoming, AIAA Journal Structural Dynamics, 1978).

(8) Ref. (5), p.16, Table I.